Appl Phys A (2008) 93: 881–884
DOI 10.1007/s00339-008-4752-3

Applied Physics A
Materials Science & Processing

Nanolithography using high transmission nanoscale ridge aperture probe

Nicholas Murphy-DuBay · Liang Wang · X. Xu

Received: 12 October 2007 / Accepted: 9 April 2008 / Published online: 27 June 2008

Abstract Nanoscale ridge apertures provide a highly confined radiation spot with a high transmission efficiency when used in the near field approach. The radiation confinement and enhancement is due to the electric–magnetic field concentrated in the gap between the ridges. This paper reports the experimental demonstration of radiation enhancement using such antenna apertures and lithography of nanometer size structures. The process utilizes a NSOM (near field scanning optical microscopy) probe with a ridge aperture at the tip, and it combines the nonlinear two photon effect from femtosecond laser irradiation to achieve sub-diffraction limit lithography resolution.

PACS 07.79.Fc · 81.16.Nd · 81.16.Rf

1 Introduction

Recently, many novel lithography processes, including near field photolithography [1–5], multi-photon lithography [6], imprint lithography [7], and surface plasmon assisted nanolithography [8] have been developed to improve the lithography resolution. Many of these processes are mask-less processes and can be used with a wide variety of substrates. For probe lithography, it comes in both aperture [9] and apertureless [10] configurations. Femtosecond lasers have also been used to improve the resolution by utilizing two-photon effects in the target material [11, 12]. A significant problem with the aperture probe based approach is the low transmission efficiency of a sub-diffraction limit aperture [13]. Recently, ridge apertures have shown to both increase the transmission efficiency and decrease the spot size in optical lithography [14, 15]. In this paper, we outline experiments combining ridge aperture NSOM probes and femtosecond laser two-photon approaches for lithography applications.

N. Murphy-DuBay · L. Wang · X. Xu (✉)
School of Mechanical Engineering, Purdue University, West Lafayette, IN 47907, USA
e-mail: xxu@ecn.purdue.edu

N. Murphy-DuBay · L. Wang · X. Xu
Birck Nanotechnology Center, West Lafayette, IN 47907, USA

2 Introduction to ridge aperture

Ridge apertures are a class of broadband apertures used frequently in microwave applications. One type of ridge aperture has a bowtie shape, which is called a bowtie aperture. As shown in Fig. 1, the bowtie aperture consists of two open arms and a small gap formed by two sharp tips pointing to each other. The two arms of the bowtie aperture have large surface areas to efficiently collect the incident radiation. Incident light polarized along the gap of the bowtie aperture generates surface currents carrying surface charge to the sharp tips of the aperture. The opposite oscillating surface charges at the tips behave like an oscillating electric dipole which radiates light through the bowtie aperture. Therefore, light with proper polarization can pass through the bowtie aperture without experiencing much intensity decay. The transmitted light is confined underneath the nanoscale gap region offering an optical resolution far beyond the diffraction limit. Detailed descriptions of the bowtie aperture theory can be found in [16–18].

In this work, bowtie apertures were specifically designed for nanolithography at the 800 nm Ti:sapphire femtosecond laser wavelength using finite difference time domain

(FDTD) numerical simulations [18] to produce the smallest spot size. The design also considered the resolution of the focus ion beam (FIB) milling technique, which is about 30 nm. A thin aluminum film is selected as the bowtie aperture material because of its small skin depth and high reflectivity. The thickness of the aluminum film was chosen to be 150 nm, which is sufficiently thick to block the light transmitted directly through the film. As shown in Fig. 2, the FDTD simulation results show that the bowtie aperture was able to achieve a sub-50 nm near field light spot with a peak field intensity as high as 39.8 times higher than the incident light at 800 nm normal illumination.

3 Experimental

The bowtie aperture probe shown in Fig. 3 is made using the following procedures. We start with the standard silicon nitride cantilevered AFM probe. A 150 nm-thick layer of aluminum film is deposited on the tip. The gold coatings on the back side of the cantilever (opposite to the pyramid) are removed by FIB milling in order to let light transmitted through the tip. FIB drilling is then used to make the bowtie aperture.

Laser light of 800 nm wavelength and a pulse width of 50 fs produced by a Ti:sapphire oscillator pumped by a solid state laser was utilized in the experiments. A halfwave plate is used to orient the polarization across the bowtie aperture gap, as required for achieving high transmission through the ridge aperture. A home-built NSOM head is used with height control and $x-y$ scanning. A diagram of the setup is shown in Fig. 4.

Shipley S1805 positive photoresist was used following standard developing procedures. A two-photon process from the 800 nm femtosecond laser pulse is expected for photoresist exposure.

4 Results and discussion

Static tests were first performed with the bowtie aperture probe to compare the experimental spot size with the predicted size. The size and depth of the spots for a bowtie

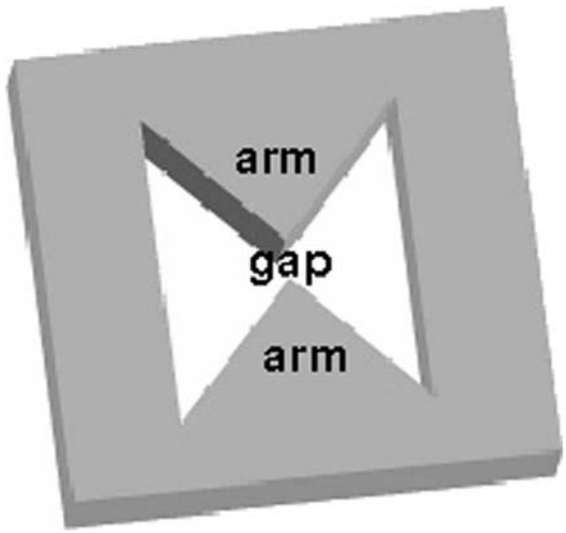

Fig. 1 Schematic drawing of the bowtie aperture

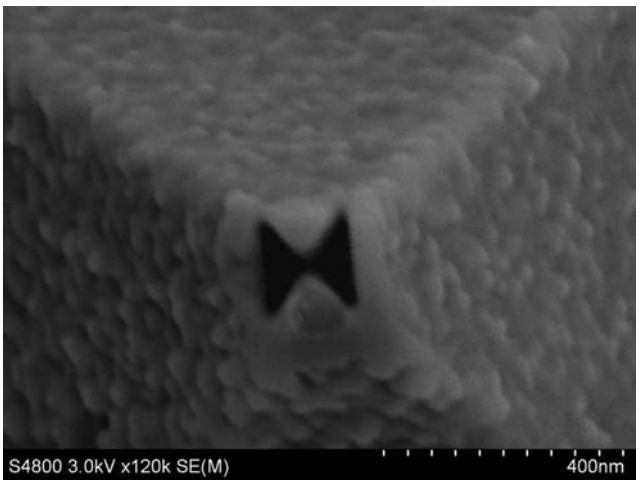

Fig. 3 SEM image of a bowtie aperture on AFM probe with inset of idealized geometry

Fig. 2 FDTD simulation result of bowtie aperture design

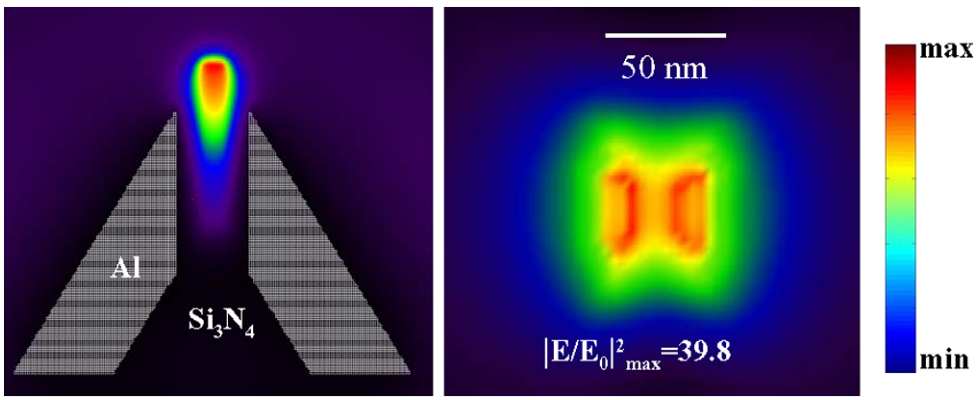

aperture with a 180 × 180 nm outline dimension and a 30 nm gap exposed at 1.5 mW exposure power on the cantilever surface were measured. The results for various dwell times are summarized in Table 1 and an AFM scan is shown in Fig. 5, with about ±10% of uncertainty in the data. The spot sizes are larger than the predicted size of sub-50 nm, and the smallest size obtained is about 60 nm, a third of the dimension of the aperture itself.

The bowtie aperture probe was then used in the NSOM system to produce line patterns. Probes with 300 × 300 nm and 100 × 100 nm square apertures were also fabricated and tested to give a baseline comparison for lines drawn by the bowtie aperture probe. A summary of the test results is shown in Table 2. The test data show that the regular apertures produced about the same size as the apertures at slow scan speed, within about ±10% uncertainty of the results. On the other hand, the smaller line width (150 nm) produced by the 300 nm aperture at high scan speed was a result of using a dose very near the threshold. The 100 nm probe did not produce any lines.

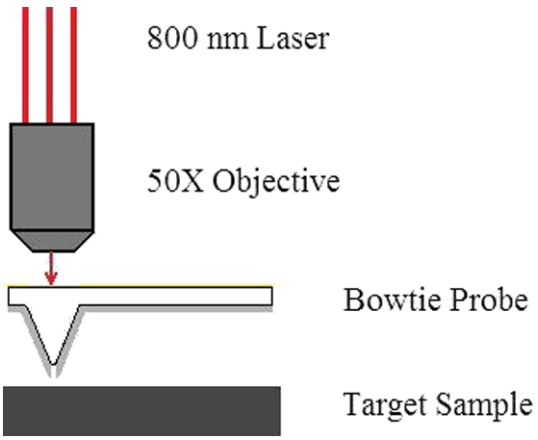

Fig. 4 Schematic diagram of the NSOM lithography setup

Table 1 Summary of static testing results for bowtie aperture probe at 1.5 mW incident power and varying dwell times

Dwell Time (s)	20	10	5	2	1
Width (nm)	127	97	75	67	61
Depth (nm)	3	3	2	2	2

The depths of the features produced by the probes were of the order of nm. This is because the transmitted field is mainly concentrated in the optical near field region and decreased quickly with the increasing distance. It is noticed that the depth of the feature produced by 100 nm is smaller than the 300 nm or bowtie probe. This is because the amount of energy coupled through the regular-shape aperture decreases quickly as the aperture size decreases.

The experimental results show that line widths and spot sizes produced by the bowtie apertures were smaller than the overall dimensions of the aperture, illustrating the light confinement. The bowtie probe produced the smallest line width, 62 nm, which is consistent with the static results. An AFM image and cross section of the smallest line obtained with the bowtie probe is shown below in Fig. 6. Further lowering the energy dose that reaches the surface of the photoresist by increasing the line speed or other means can generate a narrower line width, but with a loss in repeatability. Our current work focuses on optimizing the bowtie aperture, the bowtie probe fabrication process, and the processing parameters.

5 Conclusion

Nanolithography experiments were performed to investigate the possible improvement upon similar processes by combining probe lithography with nanoscale bowtie apertures. It was shown that this combination was able to successfully manufacture nanoscale lines below the diffraction limit. Lines with a line width of about 62 nm were produced on a positive photoresist coated sample by the bowtie apertures fabricated on an NSOM probe. The lithography results clearly show the advantages of using a bowtie aperture for probe based lithography.

Table 2 Summary of test results for the three probes showing line widths (first number) and depths (second number) in nm. Surface powers for the 300, 100, and bowtie probes were 7.9, 2.5, and 1.5 mW respectively

Speed	300 nm probe	100 nm probe	Bowtie probe
2.5 um/sec	300/8	100/1	90/4
4.5 um/sec	150/4	none	62/3

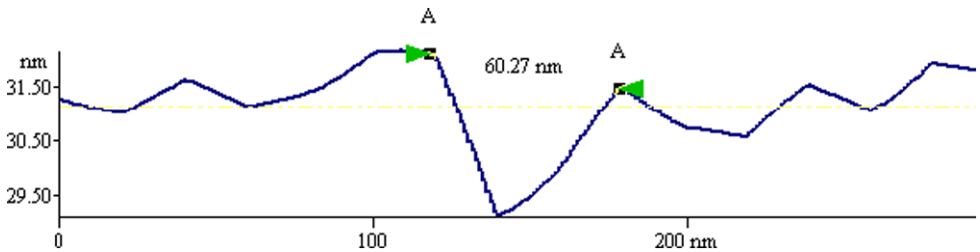

Fig. 5 AFM scan of the cross section of a hole created with static exposure of the bowtie aperture probe

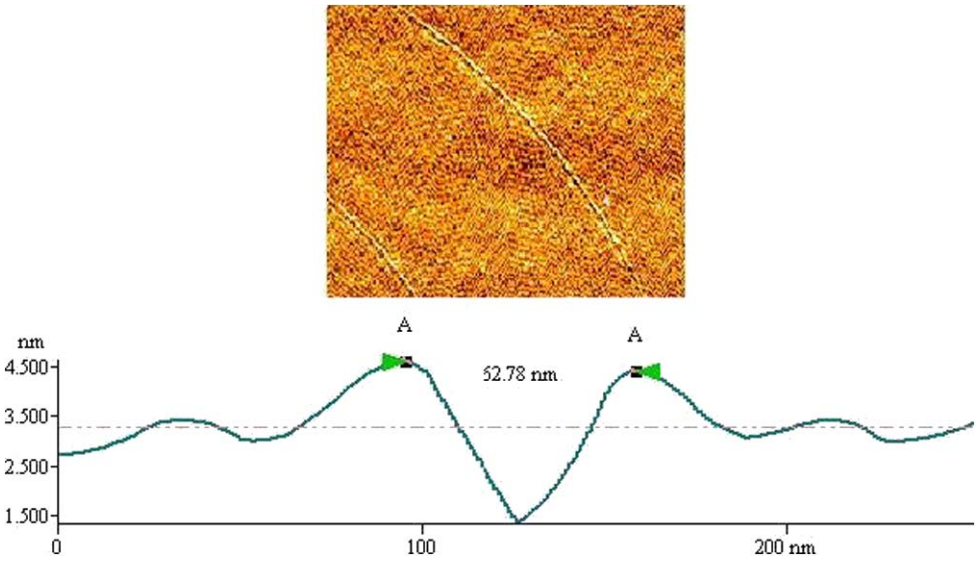

Fig. 6 AFM scan of bowtie probe curves with cross section of AFM scan results

Acknowledgements The financial support for this work by the National Science Foundation is acknowledged. The authors would also like to thank Edward Kinzel for his help with the FIB fabrication of the probes.

References

1. J. Aizenberg, J.A. Rogers, K.E. Paul, G.M. Whitesides, Appl. Phys. Lett. **71**, 3773 (1997)
2. M.M. Alkaisi, R.J. Blaikie, S.J. McNab, R. Cheung, R.S. Cumming, Appl. Phys. Lett. **75**, 3560 (1999)
3. F. Cacialli, R. Riehnb, A. Downesc, G. Latinic, A. Charasd, J. Morgadod, Ultramicroscopy **100**, 449 (2004)
4. R. Riehn, A. Charas, J. Morgado, F. Cacialli, Appl. Phys. Lett. **82**, 526 (2003)
5. R. Riehn, F. Cacialli, J. Opt. A: Pure Appl. Opt. **7**, 207 (2005)
6. S. Maruo, O. Nakamura, Sa. Kawata, Opt. Lett. **22**, 132 (1997)
7. S.Y. Chou, P.R. Krauss, P.J. Renstrom, Appl. Phys. Lett. **67**, 3114 (1995)
8. S. Davy, M. Spajer, Appl. Phys. Lett. **69**, 3306 (1996)
9. S. Kwon, P. Kim, W. Chang, J. Kim, C. Chun, D. Kim, S. Jeong, In: Proceedings of 6th International Symposium on Laser Precision Microfabrication (2005)
10. A. Tarun, M.R. Daza, N. Hayazawa, Y. Inouye, S. Kawata, Appl. Phys. Lett. **80**, 3400 (2002)
11. J. Koch, E. Fadeeva, M. Engelbrecht, C. Ruffert, H.H. Gatzen, A. Ostendorf, B.N. Chichkov, Appl. Phys. A **82**, 23 (2006)
12. W. Chang, J. Kim, S. Cho, K. Whang, Jpn. J. Appl. Phys. **45**, 2082 (2006)
13. H.A. Bethe, Phys. Rev. **66**, 163 (1944)
14. L. Wang, S.M. Uppuluri, E.X. Jin, X. Xu, Nano Lett. **6**, 361 (2006)
15. A. Sundaramurthy, P.J. Schuck, N.R. Conley, D.P. Fromm, G.S. Kino, W.E. Moerner, Nano Lett. **6**, 355 (2006)
16. K. Sendur, W. Challener, C. Peng, J. Appl. Phys. **96**, 2743 (2004)
17. E.X. Jin, X. Xu, Jpn. J. Appl. Phys. **43**, 407 (2004)
18. E.X. Jin, X. Xu, Appl. Phys. Lett. **86**, 111106 (2005)